Unregulated antigen-presenting cell activation by T cells breaks self tolerance

Jaeu Yi[a,b], Jisun Jung[a,b], Sung-Wook Hong[a,b], Jun Young Lee[a,b], Daehee Han[a,b], Kwang Soon Kim[a,b], Jonathan Sprent[c,d,1,2], and Charles D. Surh[a,b,e,1,3]

[a]Academy of Immunology and Microbiology, Institute for Basic Science, Pohang 37673, Republic of Korea; [b]Department of Integrative Biosciences and Biotechnology, Pohang University of Science and Technology, Pohang 37673, Republic of Korea; [c]Immunology Division, Garvan Institute of Medical Research, Darlinghurst, NSW 2010, Australia; [d]St. Vincent's Clinical School, University of New South Wales, Sydney, NSW 2010, Australia; and [e]Division of Developmental Immunology, La Jolla Institute for Allergy and Immunology, La Jolla, CA 92037

Contributed by Jonathan Sprent, November 28, 2018 (sent for review October 31, 2018; reviewed by Stephen M. Hedrick and Stephen C. Jameson)

T cells proliferate vigorously following acute depletion of CD4$^+$ Foxp3$^+$ T regulatory cells [natural Tregs (nTregs)] and also when naive T cells are transferred to syngeneic, nTreg-deficient *Rag1*$^{-/-}$ hosts. Here, using mice raised in an antigen-free (AF) environment, we show that proliferation in these two situations is directed to self ligands rather than food or commensal antigens. In both situations, the absence of nTregs elevates B7 expression on host dendritic cells (DCs) and enables a small subset of naive CD4 T cells with high self affinity to respond overtly to host DCs: bidirectional T/DC interaction ensues, leading to progressive DC activation and reciprocal strong proliferation of T cells accompanied by peripheral Treg (pTreg) formation. Likewise, high-affinity CD4 T cells proliferate vigorously and form pTregs when cultured with autologous DCs in vitro in the absence of nTregs: this anti-self response is MHCII/peptide dependent and elicited by the raised level of B7 on cultured DCs. The data support a model in which self tolerance is imposed via modulation of CD28 signaling and explains the pathological effects of superagonistic CD28 antibodies.

antigen-free mice | self tolerance | regulatory T cells | costimulatory molecules | autologous mixed lymphocyte reaction

Tolerance to self components involves a combination of intrathymic deletion (negative selection) of T cells with overt self reactivity and suppression by a subset of CD4 T regulatory cells (Tregs) expressing the transcription factor Foxp3 (1, 2). Absence or mutation of *Foxp3* causes a lethal syndrome of uncontrolled T cell proliferation and lymphadenopathy, as seen in *Foxp3*^{null} scurfy mice and diphtheria toxin (DT)-treated Foxp3-DTR mice; in humans, mutation of *Foxp3* leads to immune dysregulation, polyendocrinopathy, enteropathy, X-linked syndrome (3). Tregs suppress the activation and effector function of conventional CD4 and CD8 T cells through release of inhibitory cytokines, such as IL-10 and TGFβ, and by regulating costimulatory molecule expression on dendritic cells (DCs) (4, 5).

Typical Tregs are generated in the thymus [natural Tregs (nTregs)] through recognition of MHC II/self peptide ligands in the presence of IL-2 and display strong suppressive function for responses of normal T cells (6). However, optimal suppression requires an additional population of Foxp3$^+$ Tregs generated from conventional CD4 T cells in the peripheral lymphoid tissues (7). Most peripherally induced Tregs (pTregs) are induced in the lamina propria of the small and large intestine through recognition of dietary and commensal microbial antigens in the presence of TGFβ and retinoic acid synthesized by mucosal DCs (8–10), while some pTregs may be generated by tolerogenic DCs in lymph nodes (LNs) draining the skin (11). Collectively, these findings imply that the primary function of pTregs is to suppress immune responses to microbial antigens, whereas effective self tolerance may require the combined action of nTregs and pTregs (7).

The stimulus for the onset of T cell proliferation in the absence of Tregs is unclear. Uncontrolled responses to commensal microbiota could be involved, but this possibility is unlikely because lymphoproliferative disease still occurs in DT-treated Foxp3-DTR mice maintained in a germ-free (GF) environment (12). This finding does not rule out a response to food antigens. However, it does raise the possibility that lymphoproliferation in the absence of Tregs could be directed largely to self antigens. Although direct evidence on this notion is sparse, culturing T cells with autologous antigen-presenting cells (APCs) in vitro leads to low-level proliferation of naive CD4 T cells; this phenomenon is termed the auto-mixed lymphocyte reaction (auto-MLR) and represents the "background" response for T cell responses to allogeneic APCs (13–15). This response is enhanced in the absence of Tregs (14) and associated with APC activation and up-regulation of costimulatory molecules (16), implying a dysregulated response to self antigens.

Under in vivo conditions, proliferation of CD4 T cells in syngeneic irradiated hosts is weak (17) and is largely a reflection of slow MHC-dependent homeostatic proliferation induced by the elevated levels of IL-7 in lymphopenic hosts (18, 19). Far stronger proliferation occurs when naive CD4 T cells are transferred to syngeneic T cell-deficient SCID or *Rag1*$^{-/-}$ hosts (20, 21). Such fast T cell proliferation is more intense in specific-pathogen–free (SPF) than GF hosts, implying that much of the proliferation is directed to commensal microbiota (20). Nevertheless, even in GF

Significance

Removal of a subset of T cells with regulatory function (Tregs) impairs immune homeostasis and causes T cell proliferation and autoimmune disease. Using mice raised under foreign-antigen–free conditions, evidence is presented that lymphoproliferation induced by Treg cell removal is directed to self antigens rather than microbial or other foreign antigens. Based on experiments conducted both in vivo and in vitro, autoreactive T cell responses developing after Treg cell removal are directed to increased expression of costimulatory molecules (CD80, CD86) on dendritic cells, thereby leading to increased immunogenicity of self ligands.

Author contributions: J.Y., J.S., and C.D.S. designed research; J.Y., J.J., S.-W.H., J.Y.L., and D.H. performed research; K.S.K. contributed new reagents/analytic tools; J.Y. analyzed data; and J.Y. and J.S. wrote the paper.

Reviewers: S.M.H., University of California, San Diego; and S.C.J., University of Minnesota.

The authors declare no conflict of interest.

Data deposition: The raw data reported in this paper have been deposited in the Gene Expression Omnibus (GEO) database, https://www.ncbi.nlm.nih.gov/geo (accession no. GSE121882).

[1]J.S. and C.D.S. contributed equally to this work.

[2]To whom correspondence should be addressed. Email: j.sprent@garvan.org.au.

[3]Deceased October 6, 2017.

This article contains supporting information online at www.pnas.org/lookup/suppl/doi:10.1073/pnas.1818624116/-/DCSupplemental.

Published online December 31, 2018.

Rag1$^{-/-}$ hosts, a proportion of donor CD4 T cells does undergo rapid proliferation.

In SPF *Rag1*$^{-/-}$ hosts, levels of B7 (CD80, CD86) on DCs are higher than in normal mice and can be returned to normal levels by injection of purified CTLA4^{+} nTregs (22). This interesting finding is in line with the evidence that nTregs remove B7 from DCs via CTLA4 (23) and raises the possibility that the fast proliferation of normal naive T cells in *Rag1*$^{-/-}$ hosts could be precipitated by the raised density of DC B7 in these mice. However, in the SPF *Rag1*$^{-/-}$ hosts used for these studies, the fast proliferation of normal T cells is directed largely to microbial antigens rather than self antigens (see above).

To seek direct information on the stimulus for T cell proliferation induced by removal or absence of Tregs, we have investigated the fate of naive T cells transferred to antigen-free (AF) mice raised on a protein-free amino acid diet (8). The results show that, both for constitutively T-deficient *Rag1*$^{-/-}$ mice and acutely Treg-depleted DT-treated Foxp3-DTR mice as hosts, a small proportion of the donor T cells proliferates vigorously irrespective of whether these hosts are SPF, GF, or AF. This proliferation is dependent on CD28/B7 interaction and correlates with the elevation of B7 density on DCs induced by removal or absence of Tregs, and is associated with pTreg formation. These findings with AF mice correlate closely with features of the auto-MLR in vitro and indicate that the break in self tolerance occurring after Treg removal is a reflection of enhanced CD28 signaling in response to elevated B7 expression.

Results

T Cell Proliferation Following Treg Depletion Is Directed Largely to Self Antigens. As mentioned above, transfer of naive T cells to *Rag1*$^{-/-}$ hosts induces a combination of slow lymphopenia-induced proliferation (LIP) in response to the raised levels of IL-7 in these hosts plus fast proliferation to microbial antigens (18, 19). This latter finding is illustrated in Fig. 1*A*. Here, with transfer of a small number (1×10^6) of Cell Trace Violet (CTV)-labeled purified naive (CD44^{lo}CD62L^{hi}) B6 CD4 T cells to SPF *Rag1*$^{-/-}$ hosts, these Treg cell-depleted donor T cells showed a conspicuous population of expanded CTV^{-} T cells in LN and spleen at day 7 after transfer, indicating substantial expansion of a subset of the donor T cells. Confirming prior findings (20), this pattern of fast proliferation was less marked in GF *Rag1* $^{-/-}$ hosts. Nevertheless, fast proliferation of donor T cells was clearly present in these mice, indicating a response directed either to food antigens or self antigens. Significantly, an essentially identical pattern of fast proliferation applied in AF mice raised on an amino acid (protein-free) diet (Fig. 1*A*). These findings therefore indicate that fast proliferation of donor T cells in GF and AF *Rag1*$^{-/-}$ hosts reflects an unregulated immune response directed to self antigens. In SPF *Rag1*$^{-/-}$ hosts, by contrast, the much larger component of fast proliferation is presumably driven largely by commensal microbiota. In line with this notion, total cell yields in the lymphoid organs were far lower in spleen and mesenteric lymph nodes (MLNs) of T cell-injected GF and AF mice than in SPF mice (Fig. 1*B*). For GF hosts, that donor cell proliferation was substantially reduced by cotransfer of Tregs (Fig. 1*A*). No proliferation occurred following T cell transfer to T-sufficient normal B6 hosts.

The above findings applied to *Rag1*$^{-/-}$ hosts, that is, immunodeficient hosts lacking Tregs. Hence, the question arose whether similar findings would apply following acute depletion of Tregs, for example, in Foxp3-DTR mice (12). To investigate this question, Foxp3-DTR mice raised under SPF, GF, or AF conditions were treated with DT every 2 d for 10 d to remove Tregs (DT-Foxp3.DTR). Surprisingly, these DT-treated mice all showed prominent splenomegaly and large numbers of cells in spleen synthesizing IFNγ (Th1 cells) and/or IL-13 (Th2 cells) but not IL-17 (Th17 cells), accompanied by prominent inflammatory infiltrates

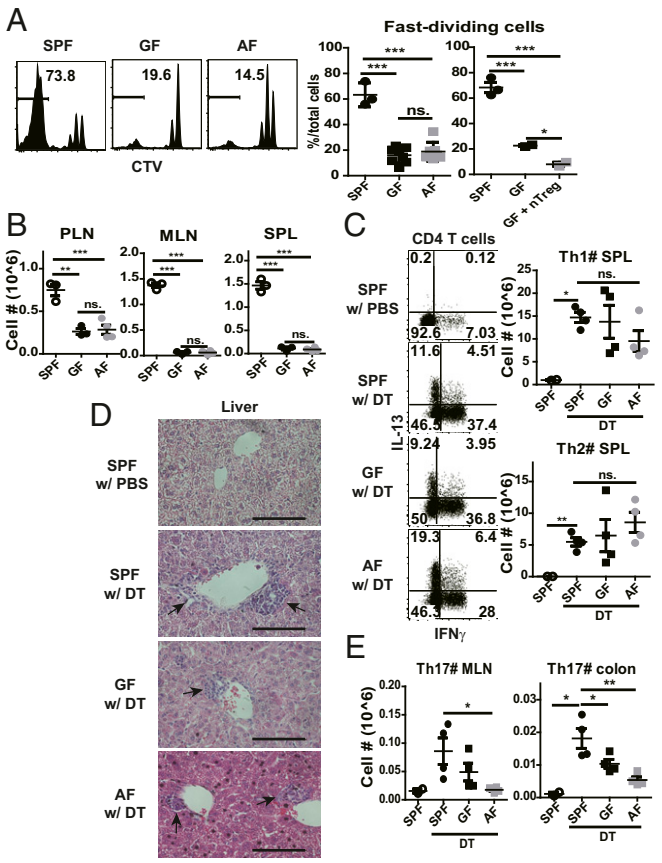

Fig. 1. T cell proliferation following Treg depletion is predominantly directed to self antigens. (*A*) Donor T cell proliferation at day 7 postinjection in lymphoid organs of SPF ($n = 3$), GF ($n = 8$), or AF ($n = 7$) *Rag1*$^{-/-}$ hosts adoptively transferred with CD44^{lo} CD62L^{hi} naive CD4 T cells from CD45.1 Foxp3-GFP mice. Also shown are the percentage of fast-dividing (CTV^{-}) T cells in SPF ($n = 3$) and GF ($n = 2$) *Rag1*$^{-/-}$ hosts injected with CD45.1 naive CD4 T cells (1×10^6) ± CD90.1 nTregs (2×10^5). Representative CTV dilution profile on CD45.1 donor T cells in peripheral LN (PLN) (*Left*), and graph for fast-dividing cells among CD45.1 total donor T cells (*Right*). (*B*) Total donor T cell numbers in PLN, mesenteric LN (MLN), or spleen (SPL) of SPF ($n = 3$), GF ($n = 3$), or AF ($n = 4$) *Rag1*$^{-/-}$ hosts injected with naive CD4 T cells at day 7 postinjection. (*C–E*) Comparison of induction of lymphoproliferative syndrome at day 10 following PBS or DT treatment of age-matched SPF, GF, or AF Foxp3-DTR mice ($n = 2$ for PBS-treated mice and $n = 4$ for DT-injected groups). (*C*) Representative FACS plots for IFNγ and IL-13 production by SPL Foxp3^{-}CD4^{+} T cells (*Left*) after 4 h of ex vivo stimulation in the presence of PMA/ionomycin and protein transport inhibitors, and total numbers of IFNγ^{+} or IL-13^{+} CD4^{+} T cells (*Right*). (*D*) H&E staining of sections of liver from Foxp3-DTR mice treated with PBS or DT, raised under SPF, GF, or AF conditions. Scale bars, 100 um. The arrows indicate lymphocyte infiltrations. (*E*) Total numbers of IL-17A–producing CD4 T cells from MLN (*Left*) or colonic lamina propria (*Right*) in mice from each group. *P* values were determined by Student's *t* test or one-way ANOVA with Newman–Keuls multiple-comparison test. Error bars show mean ± SEM. $*P < 0.05$; $**P < 0.01$; $***P < 0.001$. Note that details of materials and methods for these and other experiments are provided in *SI Appendix, Materials and Methods*.

in the liver (Fig. 1 *C* and *D*). Since these responses were undiminished in AF mice, we conclude the responses were directed predominantly to self antigens rather than foreign antigens. However, cytokine production in MLN and colonic lamina propria were lower in AF mice than in SPF or GF mice, especially for Th17 cells (Fig. 1*E*). Hence, a component of the proliferation induced by Treg depletion was directed to food and microbial antigens in the gut-associated lymphoid tissues. Nevertheless, for other organs, the bulk of the proliferation was directed to self antigens.

Adoptive T Cell Proliferation in DT-Foxp3-DTR Hosts Involves High-Affinity T Cells. To examine whether the T cells proliferating in DT-Foxp3-DTR mice arose from naive precursor cells, we adoptively transferred CTV-labeled purified populations of CD45 congenic naive CD4 or CD8 T cells into SPF Foxp3-DTR mice, followed 1 d later by repeated injection of DT to selectively deplete host Tregs. For both CD4 and CD8 T cells, host Treg depletion led to rapid proliferation of a subset of donor T cells, which expanded to form a substantial component of CTV^- cells in peripheral LN (PLN), MLN, and spleen (Fig. 2*A*). Proliferation was most prominent for donor CD4 T cells, and expanded numbers of these cells were also present in liver and the lamina propria of the small and large intestine (sLP, cLP) (*SI Appendix*, Fig. S1*A*). Treg markers on a proportion of these cells (*SI Appendix*, Fig. S1*B*) will be discussed later.

The precursor frequency of the responding T cells (*SI Appendix*, *Materials and Methods*) was quite small, namely ~1% in PLN and ~3% in MLN (*SI Appendix*, Fig. S2*A*). These estimates were close to the 4% precursor frequency reported previously for donor CD4 T cells recovered from spleen of SPF DT-Foxp3.DTR mice (24). For AF hosts, the precursor frequency was ~1–1.5% for donor cells in PLN, MLN, and spleen (*SI Appendix*, Fig. S2*B*).

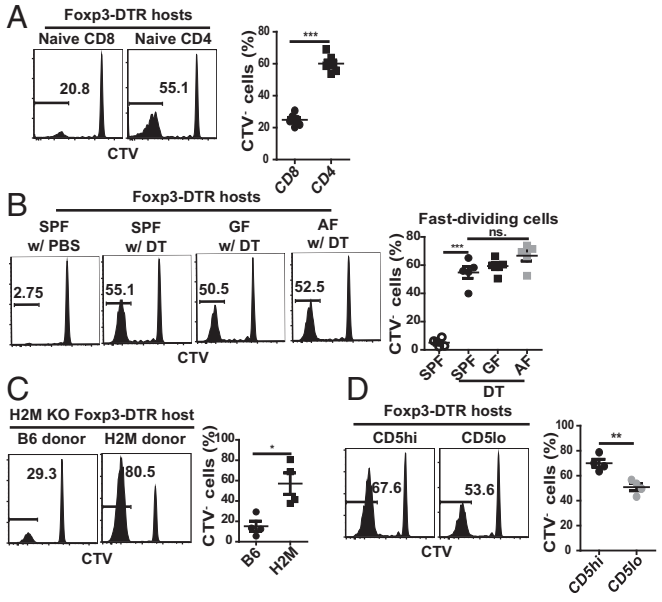

Fig. 2. Preferential proliferation of CD4 T cells with high TCR affinity for self-pMHC following Treg depletion. (*A* and *B*) Comparison of donor T cell proliferation at day 7 postinjection in Foxp3-DTR hosts adoptively transferred with 2×10^6 purified CTV-labeled $CD44^{lo}$ $CD62L^{hi}$ naive CD4 or CD8 T cells from CD45.1 Foxp3-GFP mice, followed 1 d later by DT injection. (*A*) Representative FACS plots for proliferation and graphs of percent fast-dividing cells for donor CD4 or CD8 T cells in SPF Foxp3-DTR hosts (n = 4 per each group). (*B*) Representative FACS plots for proliferation and graph of percent fast-dividing donor CD4 T cells in SPF, GF, or AF Foxp3-DTR hosts (n = 5 per each group). (*C*) $H2m^{-/-}$Foxp3-DTR hosts adoptively transferred with 2×10^6 $CD44^{lo}$ $CD62L^{hi}$ naive CD4 T cells purified from WT or $H2m^{-/-}$ Foxp3-GFP mice followed by DT injection as in *A* and *B*. Shown are representative FACS plots for proliferation and graph of percent fast-dividing donor T cells at day 10 following Treg depletion (n = 4). (*D*) Representative CTV dilution profile of donor T cells and graph of percent fast-dividing donor T cells at day 7 postinjection in Foxp3-DTR hosts adoptively transferred with 2×10^6 $CD5^{hi}$ or $CD5^{lo}$ $CD44^{lo}$ $CD62L^{hi}$ naive CD4 T cells from Foxp3-GFP mice followed 1 d later by DT injection as in *A* and *B*; upper 25% or lower 25% of naive CD4 T cells were isolated based on their CD5 expression. Shown are representative FACS plots for proliferation and graph of percent fast-dividing donor T cells (n = 4 per each group). P values were determined by Student's t test or by one-way ANOVA with Newman–Keuls multiple-comparison test. Error bars show mean ± SEM. $^*P < 0.05$; $^{**}P < 0.01$; $^{***}P < 0.001$.

In agreement with the data on precursor frequency, proliferation of donor naive CD4 T cells in PLN of Foxp3-DTR mice was as high in GF and AF hosts as in SPF hosts (Fig. 2*B*). Notably, similar results occurred with $H2M^{-/-}$ hosts, that is, mice that exclusively express self CLIP peptide/MHC II complexes (25). Thus, strong proliferation occurred when naive CD4 T cells from $H2M^{-/-}$ mice were transferred to autologous DT-treated $H2M^{-/-}$ SPF Foxp3-DTR mice (Fig. 2*C*). Hence, following Treg removal, strong proliferation by donor naive CD4 T cells was elicited by contact with a single ubiquitously expressed self peptide.

T cell responsiveness to self antigens is known to involve a range of TCR affinities and correlates with relative expression of CD5 (26, 27). Surprisingly, it was reported that donor T cell proliferation in DT-treated SPF Foxp3-DTR hosts was higher for $CD5^{lo}$ than $CD5^{hi}$ cells (24). In our hands, however, proliferation of donor CD4 T cells was significantly less with $CD5^{lo}$ cells than $CD5^{hi}$ cells (Fig. 2*D*). Further evidence came from studies with T cells from Nur77-GFP reporter mice (28). Thus, CD4 T cells sorted for high Nur77 expression, that is, cells considered to have high self reactivity, gave much stronger proliferation in DT-treated Foxp3-DTR mice than T cells with low Nur77 expression (*SI Appendix*, Fig. S3 *A* and *B*). Together, these data imply that T cell proliferation induced by Treg depletion is skewed to high-affinity cells.

The above data applied to DT-Foxp3-DTR mice. Similar findings applied to T cell transfer to GF $Rag1^{-/-}$ hosts. Thus, proliferation of naive CD4 T cells was more intense for $CD5^{hi}$ than $CD5^{lo}$ cells (*SI Appendix*, Fig. S3*C*); this finding applied in spleen and MLN as well as in PLN.

APC Requirements for Inducing Anti-Self Responses. Donor T cell responses in DT-Foxp3-DTR mice were partly IL-2 dependent. Thus, IL-2 blockade had little or no effect on T cell expansion (*SI Appendix*, Fig. S3*D*) but did cause a significant decrease in Th1 and Th2 effector cell generation (*SI Appendix*, Fig. S3*E*). With regard to the role of B7, lymphoproliferation of T cells in Scurfy and DT-treated Foxp3-DTR mice is known to be strongly dependent on CD28/B7 (CD80, CD86) interaction (29, 30). In support of this finding, donor CD4 T cell proliferation in SPF DT-treated Foxp3-DTR hosts was abolished by coinjection of a mixture of anti-CD80 and anti-CD86 mAbs (*SI Appendix*, Fig. S3*F*).

In line with the capacity of Tregs to reduce B7 expression on APCs (3–5), DT treatment of SPF Foxp3-DTR mice induced a progressive increase in both CD80 and CD86 on DCs in PLN when examined at 1 wk after injection (Fig. 3*A*). Confirming previous findings (3), DT treatment also induced a marked increase in numbers of host DCs (Fig. 3*A*). Interestingly, there was prominent expansion and differentiation of these cells into $CD11b^+Ly6C^+$ inflammatory DCs (Fig. 3*B*), which correlated with the marked differentiation of host CD4 cells into Th1 and Th2 effector cells (Figs. 1*C* and 3*C*). This finding suggested that cytokine production by the effector cells may have caused an influx of DCs into LN from elsewhere, perhaps the bone marrow. Notably, impairing T–APC interaction by injecting a mixture of neutralizing mAbs against TNFα, CD40L, and ICOSL (block, referring to mAb addition in figure) prevented DC expansion and B7 up-regulation, and also blocked host CD4 T cell proliferation and differentiation into effector cells (Fig. 3 *A*–*C*). These findings in SPF DT-Foxp3.DTR mice were extended to AF DT-Foxp3.DTR mice. Here, kinetic studies showed that total numbers of PLN DCs rose sharply between days 2 and 4 after starting DT treatment and reached peak high levels around day 7 (Fig. 3*D*). In parallel, B7 levels on DCs also rose abruptly after

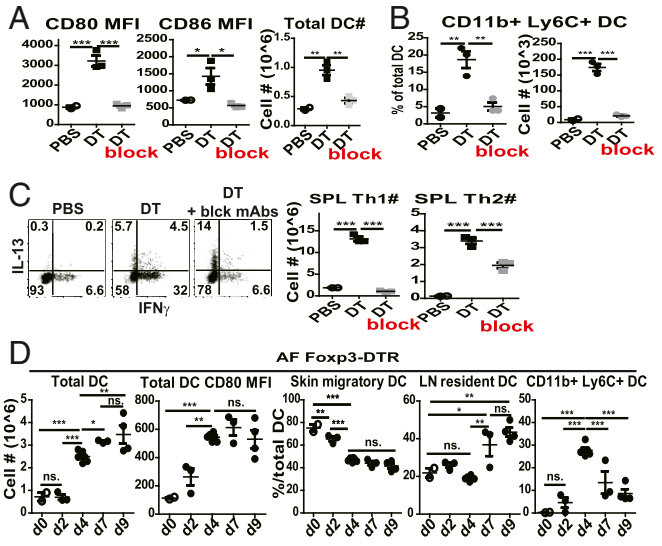

Fig. 3. DCs undergo progressive phenotypic changes following acute Treg depletion. (*A*–*C*) Foxp3-DTR mice were treated with PBS ($n = 2$), DT ($n = 3$), or DT plus a mixture of neutralizing mAbs against TNFα, CD40L, and ICOSL (block) ($n = 3$) and assayed 1 wk later. (*A*) Mean fluorescence intensity (MFI) of CD80/86 on PLN DCs (*Left*). Total numbers of PLN DCs (*Right*). (*B*) Percentages of CD11b$^+$ Ly6C$^+$ cells among PLN DCs and total numbers of PLN CD11b$^+$ Ly6C$^+$ DCs. (*C*) Representative FACS plots for IFNγ and IL-13 production by splenic CD4 T cells after 4 h of ex vivo restimulation in the presence of PMA/ionomycin and protein transport inhibitors (*Left*), and total numbers of Th1 or Th2 cells (*Right*). (*D*) PLN DC activation kinetics at day 0 ($n = 2$), day 2 ($n = 3$), day 4 ($n = 6$), day 7 ($n = 3$), and day 9 ($n = 4$) following DT injection of AF Foxp3-DTR mice. Numbers of total PLN DCs, MFI of CD80 on total PLN DCs, and percent graphs of skin migratory DCs, LN-resident DCs, or CD11b$^+$ Ly6C$^+$ DCs among total PLN DCs. Gating on TCRβ$^-$ B220$^-$ Thy1.2$^-$ NK1.1$^-$ Ly6C$^-$ cells, MHCII^{hi} CD11c^{int} cells were defined as skin migratory DCs, and MHCII^{int} CD11c^{hi} cells as LN-resident DCs. *P* values were determined by one-way ANOVA with Newman–Keuls multiple-comparison test. Error bars show mean ± SEM. $*P < 0.05$; $**P < 0.01$; $***P < 0.001$.

day 2 to reach peak levels by day 4. With regard to phenotype, the DCs at the start of DT treatment (day 0) consisted largely of MHCII^{hi} CD11c^{int} skin migratory DCs, with smaller numbers of MHCII^{int} CD11c^{hi} LN-resident DCs and no detectable CD11b$^+$ Ly6C$^+$ inflammatory DCs (Fig. 3*D*). After DT treatment, inflammatory DCs began to appear on day 2 and reached a peak of ∼30% of total DCs on day 4 before declining to ∼10% of DCs around day 9. These findings implied that the sharp increase in total DCs induced by DT treatment was due in part to an influx of inflammatory DCs but also involved local expansion of LN DC populations.

In the above experiments with DT-Foxp3.DTR mice, B7 on host DCs was at a low physiological level at the time of donor T cell injection and then rose progressively after DT treatment, which was initiated at 1 d after T cell injection. The situation in GF *Rag1*$^{-/-}$ hosts was somewhat different. In these hosts, reflecting the constitutive absence of Tregs, the density of B7 was significantly higher than in normal mice (Fig. 4*A*), presumably reflecting the lack of transendocytosis of B7 by Tregs (23). Confirming previous findings (22), injection of Treg-containing populations of CD4 T cells into GF *Rag1*$^{-/-}$ hosts reduced B7 expression to the level found in normal mice (Fig. 4*B*). By contrast, as with DT treatment of Foxp3.DTR mice, injection of purified naive CD4 T cells into GF *Rag1*$^{-/-}$ hosts caused a marked increase in B7 expression and the appearance of a high proportion of inflammatory DCs at 1 wk posttransfer (Fig. 4*B*). The opposing effects of injecting Tregs versus naive CD4 T cells on B7 (CD86) expression on host DCs was confirmed by RNA-sequencing (RNA-seq) analysis: Tregs reduced CD86 RNA, whereas naive CD4 cells increased CD86 RNA along with elevation of monocyte (CD14, Ly6C2) markers (Fig. 4*C*). With regard to kinetics, there was little or no change in host DCs for the first 5 d after naive CD4 T cell transfer (Fig. 4*D*). Thereafter, B7 expression rose progressively to reach high levels by day 12, along with an increase in total DCs; as in DT-Foxp3.DTR mice, there was a prominent influx of inflammatory DCs, which reached a peak on day 8 and then declined.

Collectively, these findings indicated that Treg depletion not only increased B7 expression on host DCs but caused these cells

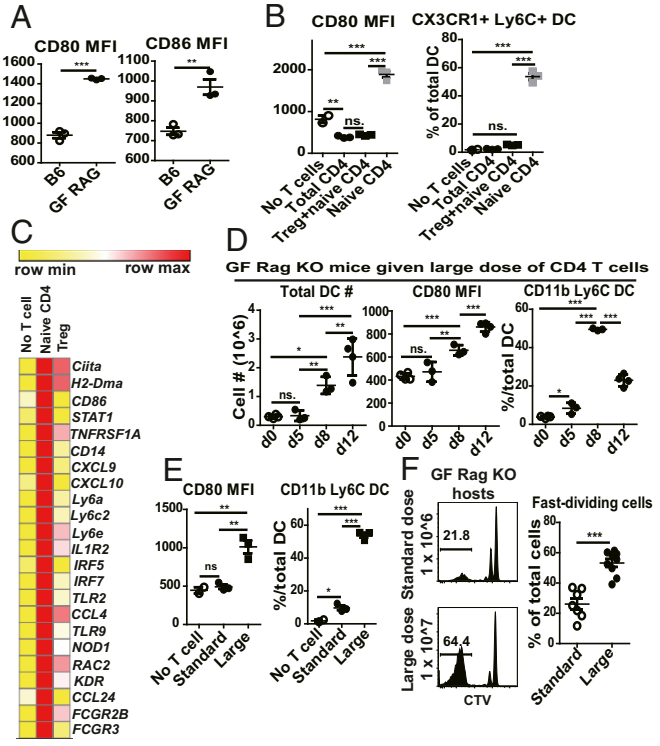

Fig. 4. DCs undergo progressive activation following Treg-depleted CD4 T cell transfer into GF *Rag1*$^{-/-}$ hosts. (*A*) Mean fluorescence intensities (MFIs) of CD80 and CD86 on total PLN DCs from uninjected B6 mice ($n = 3$) or GF *Rag1*$^{-/-}$ mice ($n = 3$). (*B*) Comparison of PLN DC populations in GF *Rag1*$^{-/-}$ hosts at day 7 following transfer of CD4 T cell populations, namely total CD4 T cells (5×10^6) ($n = 3$), Tregs (5×10^5) plus CD44^{lo} CD62L^{hi} naive CD4 T cells (4×10^6) ($n = 3$), or naive CD4 T cells alone (4×10^6) ($n = 3$). Shown are MFI of CD80 on total PLN DCs (*Left*) and percentages of Ly6C$^+$ CX3CR1$^+$ DCs among PLN DCs (*Right*). (*C*) RNA-seq analysis of highly purified PLN DCs from uninjected GF *Rag1*$^{-/-}$ mice, and GF *Rag1*$^{-/-}$ mice injected 1 wk before with CD44^{lo} CD62L^{hi} naive CD4 T cells or purified Tregs; each RNA sample was combined from more than five mice. Shown are heatmap comparisons of representative genes. (*D*) PLN DC phenotype in GF *Rag1*$^{-/-}$ hosts following injection of a large dose (5×10^6) of CD44^{lo} CD62L^{hi} naive CD4 T cells from CD45.1 Foxp3-GFP mice; recipients were assayed at day 0 ($n = 4$), day 5 ($n = 3$), day 8 ($n = 3$), and day 12 ($n = 4$) postinjection. Shown are total PLN DC numbers, CD80 MFI on total PLN DCs, and percentages of CD11b$^+$ Ly6C$^+$ cells among total PLN DCs. (*E* and *F*) PLN DC phenotype and donor T cell proliferation in GF *Rag1*$^{-/-}$ hosts at day 7 following injection of a standard dose (1×10^6) or large dose (1×10^7) of CTV-labeled CD44^{lo} CD62L^{hi} naive CD4 T cells from CD45.1 Foxp3-GFP mice. (*E*) Shown are CD80 MFI on total PLN DCs and percentages of CD11b$^+$ Ly6C$^+$ cells among total PLN DCs (no T cell injection, $n = 2$; standard dose injection, $n = 3$; large dose injection, $n = 3$). (*F*) CTV dilution profile on donor T cells (*Left*). Percentages of fast-dividing T cells (*Right*) (standard dose, $n = 7$; large dose, $n = 9$). *P* values were determined by Student's *t* test or by one-way ANOVA with Newman–Keuls multiple-comparison test. Error bars show mean ± SEM. $**P < 0.01$; $***P < 0.001$.

to become overtly activated and also to replicate via interaction with autologous normal CD4 T cells. Hence, there was a sequence of bidirectional T/APC signaling, resulting in expansion and differentiation of both T cells and DCs.

In considering the consequences of T/APC interaction, it should be noted that, in GF *Rag1*$^{-/-}$ hosts, the overt activation of host DCs applied only with a relatively large dose of 5×10^6 naive CD4 T cells, which was fivefold higher that the standard dose of 1×10^6 cells used to measure T cell proliferation (Fig. 1*A*). This difference was important because, unlike a large dose (1×10^7), injection of the small dose (1×10^6) of naive CD4 T cells caused little or no change in B7 expression on host DCs at day 7 and only a small influx of inflammatory DCs (Fig. 4*E*). This T cell dose-dependent activation of host DCs had a marked effect on the intensity of the proliferative response. Thus, fast proliferation was much more prominent with injection of large numbers of T cells than with small numbers (Fig. 4*F*). The functional consequences of this difference are considered below.

nTreg Depletion Leads to pTreg Generation. With Foxp3.DTR mice, DT treatment ablates all host Tregs, including pTregs. With adoptive transfer of normal T cells into these hosts, however, DT treatment is unable to delete pTregs developing from the donor T cells. In this respect, studies with T cells from Foxp3-GFP reporter mice showed that pTreg generation from donor-derived T cells was observed in virtually all of the above experiments involving transfer of naive CD4 T cells to DT-Foxp3.DTR mice. With normal B6 CD4 T cells, this finding applied equally to SPF, GF, and AF mice. For these T cells, and also *H2M*$^{-/-}$ cells, pTreg conversion applied to 10–20% of donor-derived cells (Fig. 5*A*). Notably, pTreg generation was heavily skewed to high-affinity CD4 T cells, being much higher for CD5^{hi}/Nur77^{hi} than CD5^{lo}/Nur77^{lo} B6 cells (Fig. 5*B*); and was associated with CTLA-4 up-regulation in multiple sites, including nonlymphoid tissues (*SI Appendix*, Fig. S1*B*). In agreement with the evidence that pTreg generation is TGFβ dependent (31), pTreg formation was low or absent with injection of anti-TGFβ mAb, or when donor T cells were prepared from double-negative (DN) TGFβRII mice (Fig. 5*C*). Functionally, the pTregs displayed suppressive function as indicated by their capacity to inhibit the activation of endogenous CD8 and CD4 T cells when they were retransferred into secondary DT-treated Foxp3-DTR hosts (*SI Appendix*, Fig. S4*A*). Their suppressive function was somewhat less potent than that of nTregs prepared from normal mice, but both Treg populations were able to prevent the induction of liver pathology (*SI Appendix*, Fig. S4*B*).

Generation of donor-derived pTregs in DT-Foxp3.DTR hosts applied irrespective of the number of T cells injected. The situation in *Rag1*$^{-/-}$ hosts was different. Here, the striking finding was that pTreg generation only occurred if relatively large numbers of T cells (1×10^7) were injected (Fig. 5*D*), that is, numbers sufficient to induce strong host DC activation (Fig. 4*E*). The data in these two models are thus in agreement with evidence that pTreg generation is strictly B7 dependent (32).

Collectively, the above studies in DT-Foxp3-DTR and *Rag1*$^{-/-}$ mice showed that depletion or absence of Tregs in vivo enabled a subset of high-affinity CD4 T cells to mount B7-dependent overt responses to self antigens associated with pTreg formation. Accordingly, similar findings would be expected to occur in vitro if naive T cells and DCs were cultured together in the absence of Tregs. This issue was addressed by studying T cell proliferation in the auto-MLR.

Features of the Auto-MLR in Vitro. As discussed earlier, the auto-MLR is the "background" level of proliferation seen when T cells are cultured with allogeneic versus syngeneic APCs in vitro (13, 15). As illustrated by the response of B6 (H2b) naive CD4 T cells to BALB/c (H2d) FACS-purified CD11c$^+$ MHCII$^+$

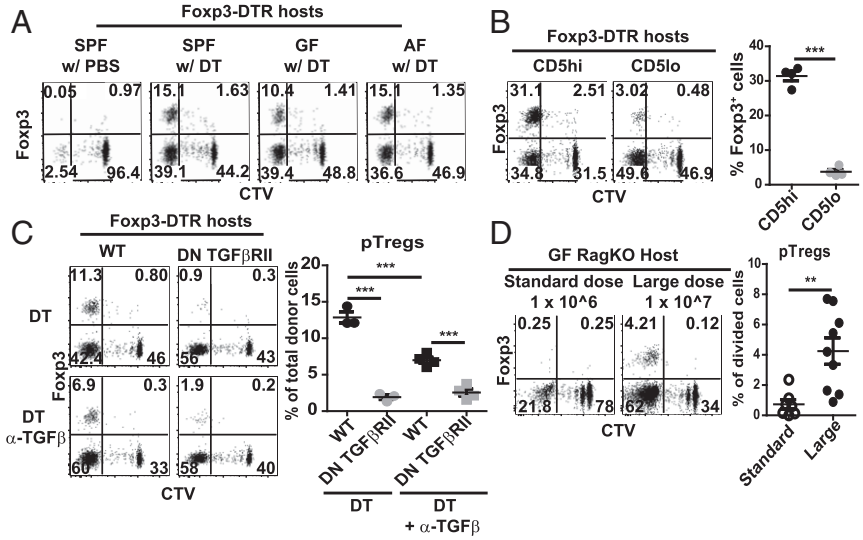

Fig. 5. A fraction of dividing CD4 T cells differentiates into pTregs following Treg depletion. (*A*) Representative FACS plots for day 7 proliferation and Foxp3-GFP expression on donor CD4 T cells in SPF, GF, or AF Foxp3-DTR hosts adoptively transferred with 2×10^6 CD44^{lo} CD62L^{hi} naive CD4 T cells from Foxp3-GFP mice followed 1 d later by DT injection as in Fig. 2*B*. (*B*) Representative CTV dilution and Foxp3-GFP expression profiles on donor T cells at day 7 postinjection in Foxp3-DTR hosts adoptively transferred with 2×10^6 CD5^{hi} or CD5^{lo} CD44^{lo} CD62L^{hi} naive CD4 T cells from Foxp3-GFP mice followed 1 d later by DT injection as in Fig. 2*D*. (*C*) Effect of TGFβ on pTreg generation was measured by injecting Foxp3-DTR mice with a mixture of 1×10^6 CD90.1 WT naive CD4 T cells and 1×10^6 CD45.1 CD4 DN TGFβRII naive CD4 T cells, both from Foxp3.GFP donors, followed 1 d later by Treg depletion; subsequently, host mice were treated with DT or DT plus anti-TGFβ mAbs. Shown are representative FACS plots for proliferation and Foxp3-GFP expression on donor T cells (*Left*), and percentages of Foxp3-GFP$^+$ cells on total donor T cells at day 7 (*Right*) (n = 3–4). (*D*) pTreg induction was compared in GF *Rag1*$^{-/-}$ hosts at day 7 following injection of a standard dose (1×10^6; n = 7) or large dose (1×10^7; n = 9) of CTV-labeled CD44^{lo} CD62L^{hi} naive CD4 T cells from CD45.1 Foxp3-GFP mice. Shown are representative FACS plots for CTV dilution and Foxp3-GFP expression on donor T cells (*Left*), and percentage of Foxp3-GFP$^+$ cells on divided T cells (*Right*). *P* values were determined by Student's *t* test. Error bars show mean ± SEM. $^{**}P < 0.01$; $^{***}P < 0.001$.

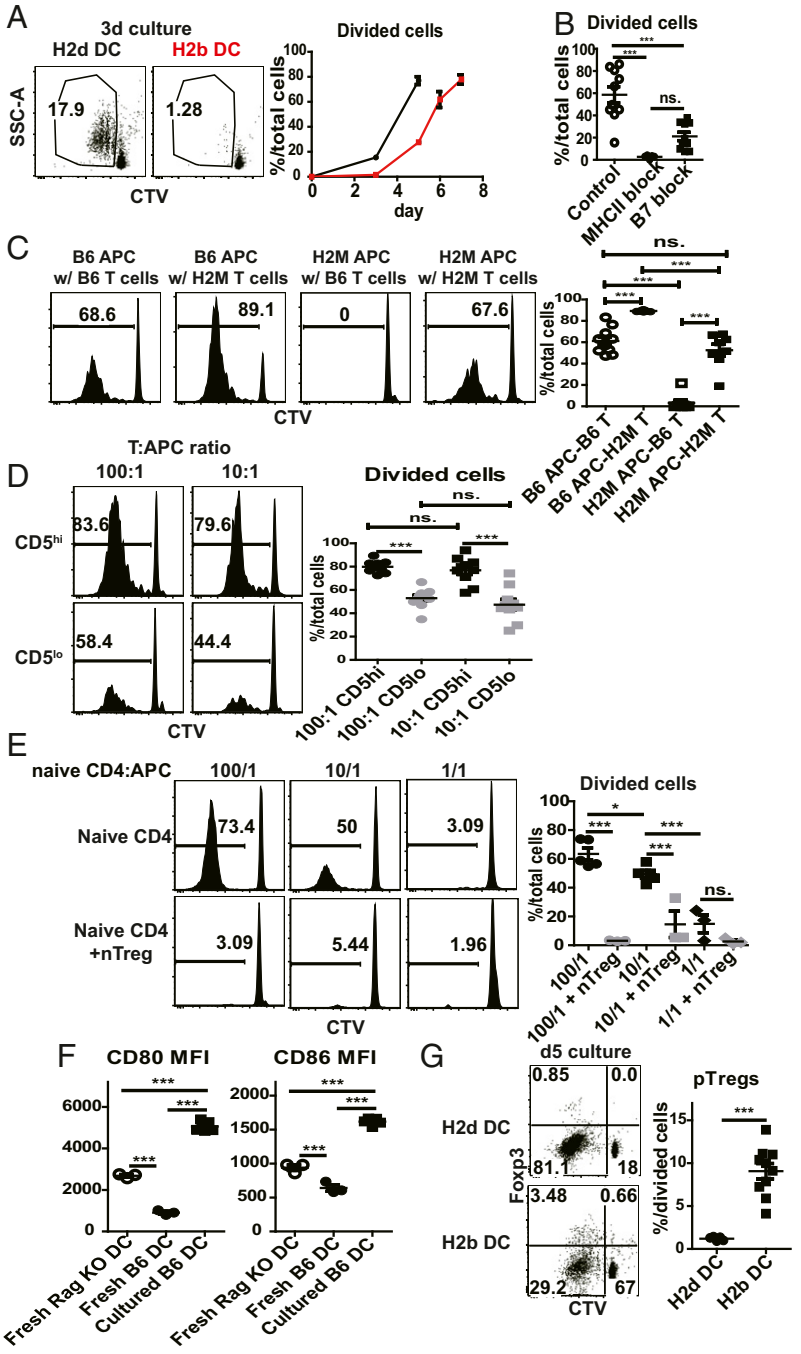

Fig. 6. MHCII ligands plus raised B7 levels induce proliferation of naive CD4 T cells in auto-MLR. Shown are auto-MLR following coculture of syngeneic purified CD11c^{+} MHCII^{+} PLN DCs with CTV-labeled CD44^{lo} CD62L^{hi} B6 naive CD4 T cells from Foxp3-GFP mice in vitro. (*A*) Comparison of coculturing 1×10^5 B6 (H2b) naive CD4 T cells with 5×10^3 BALB/C (H2d) or B6 (H2b) PLN DCs. Shown are representative FACS plots of proliferation of T cells in 3-d culture (*Left*), and percentage of divided cells at various time points (*Right*). (*B*) Effect of MHCII or B7 blockade on auto-MLR. A total of 5×10^3 PLN B6 DCs was cocultured with 1×10^5 B6 naive CD4 T cells in the presence of PBS ($n = 10$), MHCII blocking mAb (10 μg/mL Y3P; $n = 5$), or B7 (CD80 + CD86) blocking mAbs (5 ug/mL 1G10 and GL-1; $n = 10$) for 7 d. Shown is percentage of divided cells for each group. (*C*) Auto-MLR for 7 d following coculture of 1×10^4 GF unseparated *Rag1*$^{-/-}$ PLN cells (B6 APCs) or 1×10^4 *H2m*$^{-/-}$ *Rag1*$^{-/-}$ PLN cells (H2M APCs) with 1×10^5 CTV-labeled naive CD4 T cells from B6 Foxp3-GFP mice or from *H2m*$^{-/-}$ Foxp3-GFP mice ($n = 8$~10). Shown are representative CTV histogram of cocultured T cells (*Left*) and percentages of divided cells among total cocultured T cells (*Right*). (*D*) Auto-MLR for 7 d with coculture of 1×10^4 B6 APCs with 1×10^6 or 1×10^5 CTV-labeled CD5^{hi} or CD5^{lo} B6 naive CD4 T cells from Foxp3-GFP mice (100/1, or 10/1 T:APC ratio; $n = 10$). For purification, upper 25% or lower 25% of naive CD4 T cells were purified for CD5 expression. Shown are representative histogram for CTV-dilution profile of total cocultured T cells (*Left*) and percentages of CTV^{-} cells of total cocultured T cells (*Right*). (*E*) Suppressive effect of nTregs on auto-MLR. Total of 1×10^6, 1×10^5, or 1×10^4 CD45.1 B6 naive CD4 T cells were cocultured with 1×10^4 B6 APCs for 8 d in the absence ($n = 5$) or presence ($n = 3$) of CD90.1-marked nTregs. The ratio of naive T cells (CD45.1):nTregs (CD90.1) was 2:1 in each situation. Shown are representative histogram of CTV dilution on cocultured CD45.1 T cells (*Left*) and percentages of CTV^{-} cells (*Right*). (*F*) Shown are mean fluorescence intensities (MFIs) of CD80 and CD86 on cultured DCs when purified PLN DCs from B6 mice were incubated alone for 24 h. CD80 and CD86 levels of PLN DCs from fresh *Rag1*$^{-/-}$ or B6 mice are shown as controls. (*G*) Comparison of pTreg induction when 1×10^5 B6 naive CD4 T cells were cocultured with 5×10^3 BALB/c (H2d) or B6 (H2b) PLN DCs for 5 d (see above) (H2d DCs, $n = 5$; H2b DCs, $n = 10$). *P* values were determined by Student's *t* test or one-way ANOVA with Newman–Keuls multiple-comparison test. Error bars show mean ± SEM. $*P < 0.05$; $**P < 0.01$; $***P < 0.001$.

PLN DCs, typical allo-MLR measured by CTV dilution were associated with strong proliferation on days 3 and 5 of culture, paralleled by only low-level proliferation with autologous B6 (H2b) PLN DCs (Fig. 6*A*). At later stages of culture, the allo-MLR declined due to cell overcrowding in the cultures. However, the auto-MLR with B6 DCs increased progressively thereafter and reached quite high levels by day 7 (Fig. 6*A*). This response was abolished by addition of either anti-B7 or anti-MHCII mabs (Fig. 6*B* and *SI Appendix*, Fig. S5*E*) and did not occur with $H2M^{-/-}$ DCs (Fig. 6*C*), implying a polyclonal response to MHCII-associated self peptides. Significantly, as in vivo, the auto-MLR was skewed to high-affinity T cells; thus, responses were higher with $CD5^{hi}$ than $CD5^{lo}$ B6 T cells (Fig. 6*D*). Also, as in vivo, $H2M^{-/-}$ naive CD4 T cells proliferated well in vitro to autologous $H2M^{-/-}$ DCs (Fig. 6*C*); unlike in vivo (Fig. 2*C*), these DCs were nonstimulatory for B6 T cells, perhaps reflecting the absence of DC expansion under in vitro conditions.

The above findings applied to responses by purified naive CD4 T cells. Notably, responses were absent or greatly reduced if naive CD4 cells were supplemented with even small numbers of Tregs (Fig. 6*E*). This finding focused attention on the stimulus for the auto-MLR and the role of B7. On this point, it is well documented that culturing DCs in vitro causes spontaneous up-regulation of B7 (33). In accordance with this finding, culturing DCs alone in culture for 1 d caused prominent up-regulation of B7 (Fig. 6*F*). Since proliferation was blocked by B7 blockade, the data indicated that, as in vivo, the in vitro response was directed to self MHCII ligands and initiated by elevated expression of B7 on DCs.

With regard to pTreg formation, in agreement with previous studies (34) the strong proliferation in the allo-MLR directed to BALB/c DCs on day 5 of culture was not associated with pTreg generation (Fig. 6*G*). By contrast, pTreg formation was clearly detectable in the delayed response to autologous B6 DCs. In accordance with the evidence that pTreg generation is TGFβ dependent (31), pTreg formation in the cultures was minimal with TGFβ-unresponsive DN TGFβRII CD4 T cells as responder cells (*SI Appendix*, Fig. S5*A*); interestingly, the cultured DCs showed elevated expression of the TGFβ precursor LAP (*SI Appendix*, Fig. S5*B*), implying that DCs were the main source of TGFβ in the cultures.

The extent of pTreg generation depended on the T/DC ratio in the cultures (*SI Appendix*, Fig. S5*C*). Thus, at a high 100/1 ratio, T cell proliferation was strong but associated with only low pTreg induction, whereas a lower 10/1 ratio led to weaker proliferation but higher pTreg induction. Notably, B7 levels on DCs were higher in the 100/1 than the 10/1 ratio cultures (*SI Appendix*, Fig. S5*D*); moreover, pTreg induction in the 100/1 cultures increased with partial B7 blockade (*SI Appendix*, Fig. S5*E*). These findings are consistent with the view that pTreg formation is favored when CD28/B7 signaling is intermediate rather than strong (35). As with partial B7 blockade, pTreg formation was enhanced by the presence of nTregs. Thus, with Foxp3-GFP–marked naive CD4 T cells as responder cells, the few divided T cells in the cultures suppressed by addition of nTregs (Fig. 6*E*) were nearly all pTregs.

With regard to in vivo relevance, it was mentioned earlier that pTreg generation in vivo correlated with an influx of inflammatory DCs into LN. Notably, of the three populations of DCs found in PLN of DT-treated Foxp3.DTR mice, the subset of $Ly6C^{+}$ $CD11b^{+}$ inflammatory DCs was the most effective at generating pTregs in vitro (*SI Appendix*, Fig. S5*F*); this finding correlated with higher LAP and lower MHCII on the inflammatory DCs (*SI Appendix*, Fig. S6). These findings with inflammatory DCs in vitro were thus consistent with the strong pTreg generation observed in DT-Foxp3.DTR mice.

Collectively, the in vitro data closely recapitulate the self ligand-driven responses observed in Treg-depleted mice. In the case of pTregs, the data support the view that pTreg formation is favored by relatively weak TCR signaling combined with moderate CD28/B7 signaling (36). This scenario raises the question whether the conspicuous generation of pTregs that accompanies unregulated responses to self ligands could serve to protect the host against pathology. This question is addressed below.

Role of pTreg in Suppressing Autologous T Cell Responses in Vivo. To investigate the protective function of pTreg generation, naive CD4 T cells were transferred to SPF versus GF $Rag1^{-/-}$ mice. The host mice were then left for several weeks before examining the mice for pathology. With T cell transfer to control SPF $Rag1^{-/-}$ hosts, rapid proliferation of the donor T cells to the host microbiota was associated with weight loss and the appearance of inflammatory cells in the liver and colon at 3 wk posttransfer (Fig. 7 *A* and *B*); as expected from previous studies (37), the onset of weight loss and inflammatory disease failed to occur following coinjection of naive T cells and Tregs (Fig. 7*B*), indicating an important protective role of nTregs in preventing disease. For GF $Rag1^{-/-}$ hosts, however, injection of the same standard low dose of 1×10^6 naive CD4 cells without Tregs failed to cause either weight loss or pathology in the liver or colon. Interestingly, pTreg induction by the 1×10^6 donor CD4 T cells, although undetectable at 1 wk posttransfer (Fig. 5*D*), was clearly apparent by 3 wk (Fig. 7*C*) and correlated with B7 up-regulation and a late influx of DCs into PLN.

This finding raised the question whether pTreg generation accounted for the lack of pathology in the host mice. To examine this question, GF $Rag1^{-/-}$ mice were injected with naive CD4 T cells prepared from Foxp3-DTR mice and then treated with DT at 3 wk to prevent pTreg formation. Notably, this treatment augmented proliferation of the donor T cells and induced significant pathology in the liver by 4 wk posttransfer (Fig. 7 *D* and *E*). In marked contrast, no pathology was seen when DT was not injected (Fig. 7*E*). Hence, these findings indicated that the lack of pathology in constitutively Treg-deficient GF $Rag1^{-/-}$ hosts injected with naive T cells reflected differentiation of the donor cells into a protective population of pTregs.

Discussion

A central finding in this paper is that the severe pathology seen after Treg depletion is directed largely to self antigens rather than to microbial or food antigens. For DT-Foxp3-DTR mice, this conclusion follows from the observation that the prominent lymphoproliferation and effector T cell generation occurring in these mice was as intense in AF mice as in GF mice. However, pathology was even more intense in SPF DT-Foxp3-DTR mice, especially in the mucosal immune system, indicating that in these mice the response to self antigens is accompanied by a concomitant strong response to gut microbial antigens. For AF mice, strong T cell proliferation in DT-Foxp3-DTR hosts was conspicuous after adoptive transfer of autologous naive CD4 T cells. Interestingly, for short-term adoptive responses, the intensity of the proliferative response in AF, GF, and SPF mice was indistinguishable. Here, proliferation of naive T cells was mediated largely by CD4 rather than CD8 T cells and was accompanied by strong generation of Th1 and Th2 effector cells and inflammatory infiltration of the liver. Significantly, proliferation was mediated predominantly by T cells with high intrinsic self MHC reactivity, as indicated by their high expression of CD5 and Nur77. As for typical responses to foreign antigens, the response to self ligands was B7 and MHC dependent. These findings applied to polyclonal B6 T cells.

As in DT-Foxp3-DTR mice, transferring naive CD4 T cells to $Rag1^{-/-}$ mice caused rapid proliferation of a proportion of the donor cells. Confirming previous findings (20), fast proliferation of donor naive CD4 T cells was weaker in GF than

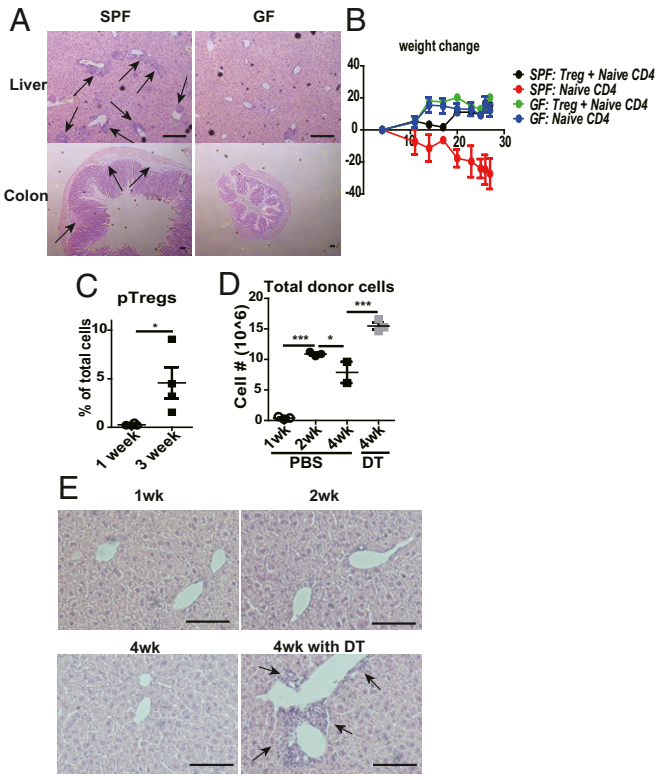

Fig. 7. pTregs suppress autologous T cell responses in vivo. (*A* and *B*) Comparison of induction of lymphoproliferative disorder in SPF or GF *Rag1*$^{-/-}$ hosts upon transfer of 1 × 10^6 CD44^{lo} CD62L^{hi} naive CD4 T cells from CD45.1 Foxp3-GFP mice. (*A*) H&E staining of sections of liver and colon at day 21 after injection (n = 4 per each). Scale bars, 100 μm. The arrows indicate lymphocyte infiltrations. (*B*) Graph for weight change percentages of SPF or GF *Rag1*$^{-/-}$ hosts after transfer of indicated T cell populations. SPF and GF *Rag1*$^{-/-}$ hosts (n = 2–3) were injected with naive CD4 T cells (1 × 10^6) alone or a mixture of naive CD4 T cells (1 × 10^6) and purified Tregs (2 × 10^5). (*C*) Percentages of Foxp3$^+$ cells among donor T cells at day 7 (n = 4) or day 21 (n = 4) in the GF *Rag1*$^{-/-}$ hosts injected with 1 × 10^6 CD44^{lo} CD62L^{hi} naive CD4 T cells from CD45.1 Foxp3-GFP mice. (*D* and *E*) Effect of depleting pTregs in GF *Rag1*$^{-/-}$ hosts adoptively transferred with 1 × 10^6 CD44^{lo} CD62L^{hi} naive CD4 T cells from Foxp3-DTR mice. Host mice were analyzed at 1 wk (n = 3), 2 wk (n = 3), or 4 wk (n = 2) posttransfer. Where indicated, DT was administered during the last week (n = 3). (*D*) Shown are total donor T cell numbers in spleen. (*E*) H&E staining of liver, with arrows pointing to lymphocytic infiltrations. *P* values were determined by Student's *t* test or by one-way ANOVA with Newman–Keuls multiple-comparison test. Error bars show mean ± SEM. *P < 0.05; **P < 0.01; ***P < 0.001.

SPF *Rag1*$^{-/-}$ mice, reflecting the lack of gut antigens in GF mice. The response was clearly significant, however, and notably was the same in AF as in GF *Rag1*$^{-/-}$ mice, indicating responsiveness to self antigens rather than food antigens. Hence, in both DT-Foxp3-DTR mice and *Rag1*$^{-/-}$ mice, the lack of Tregs broke self tolerance and caused a proportion of normal T cells to become strongly responsive to autologous antigens.

Since the bulk of strongly autoreactive T cells are presumed to be destroyed by negative selection in the thymus (38), how can one explain the onset of autologous responses when Tregs are removed? Here, it should be noted that precursor frequency analysis showed that the proportion of naive CD4 T cells able to proliferate in DT-Foxp3-DTR hosts was quite low, that is, ∼1%, although this could be an underestimate because of competition for APCs by the expanding host T cells. The nature of the self ligands responsible for activating high-affinity T cells is clearly a key issue. An obvious possibility is that the target ligands are tissue-specific antigens (TSAs) entering the lymphoid tissues, and that the T cells reactive to TSAs are cells that evaded AIRE-dependent deletion in the thymus (39). The alternative possibility is that the ligands are largely ubiquitous self peptides expressed by many, perhaps all, cells including APCs. This latter notion fits well with the data shown here on the auto-MLR, that is, that contact with isolated normal syngeneic DCs in vitro was sufficient to elicit quite strong proliferative responses by syngeneic naive CD4 T cells. However, more definitive information came from the studies on DT-Foxp3-DTR *H2M*$^{-/-}$ mice, that is, mice that expressed only a single ligand, namely MHC II-bound CLIP peptide. In these mice, thymic selection to CLIP alone generates a polyclonal repertoire of normal CD4 T cell subsets, including Tregs, and normal self tolerance (25). However, when used as hosts for adoptive transfer, these Treg-depleted mice were strongly immunogenic for autologous naive *H2M*$^{-/-}$ CD4 cells and, to a lessor extent, for naive normal B6 CD4 cells. In this situation, therefore, Treg depletion led to the onset of overt CD4 T cell responsiveness to a single ubiquitous self antigen. In light of this finding, it seems likely that the anti-self responses observed here in normal DT-Foxp3-DTR and GF *Rag1*$^{-/-}$ hosts are directed largely to common self peptides rather than to TSAs. Clearly, further information on this important issue is needed.

In considering how Treg removal causes naive T cells to respond to self ligands, recent studies on superagonistic CD28SA mAb [which caused florid pathology as TGN1412 in a clinical trial (40)] are instructive. In particular, injection of CD28SA into mice was shown to elicit proliferation of normal CD4 T cells, in addition to Tregs, although only when CD4 cells maintained contact with MHCII$^+$ DCs (41). These findings imply that the covert tonic TCR signals that keep normal T cells alive in the lymphoid tissues (19, 42) can become overt following CD28 ligation and drive the cells into division. Under physiological conditions, this regulation could be controlled by the level of B7 expression on APCs. In the presence of Tregs, B7 expression on APCs is kept at a low level via CTLA4 stripping (23) and also by CTLA4-mediated STAT3 phosphorylation leading to suppression of B7 gene transcription (43); such B7 modulation causes naive T cells to remain in interphase unless they contact foreign antigens. In the absence of Tregs, however, B7 expression on APCs is known to increase (3, 22) and could thereby promote CD28 signaling in T cells contacting these APCs. Hence, for T cells with relatively high self MHC affinity, one can envisage that the slight increase in CD28 signaling in conjunction with constitutive TCR signals causes these T cells to undergo activation and begin to proliferate, thereby breaking self tolerance. This model was proposed previously to explain rapid proliferation of donor T cells transferred to SPF *Rag1*$^{-/-}$ mice (22). However, proliferation in this SPF model is known to be directed largely to microbial antigens, so it was unclear whether the data were applicable to self antigens.

The notion that self tolerance is basically a reflection of the intensity of steady-state TCR/CD28 signaling in naive T cells implies that even a small increase in B7 expression on APCs could break self tolerance and be sufficient to induce T cells to become overtly self reactive. In this respect, it was mentioned earlier that the lack of Tregs in SPF *Rag1*$^{-/-}$ mice was associated with a significant increase in DC B7 expression, which returned to normal levels following injection of Tregs (22). We confirmed this finding in GF *Rag1*$^{-/-}$ mice by the finding that elevation in B7 levels in PLN of these mice (relative to normal B6 mice) decreased to normal following injection of Treg-containing cell populations but rose markedly to high levels following transfer of naive CD4 T cells.

In view of the above findings, it seems highly likely that the anti-self response seen in GF and AF *Rag1*$^{-/-}$ mice was initiated by the above-normal B7 density on host DCs. We envisage that,

in these hosts, and also in DT-Foxp3.DTR mice, this slight increase in B7 density caused naive CD4 T cells with the highest affinity for self ligands to become overtly activated by DCs and start to divide and up-regulate costimulatory molecules such as CD40L: in turn, this response elicited DC activation and expansion, probably via CD40/CD40L interaction and cytokine production, thereby inducing further B7 up-regulation and, consequently, enhanced immunogenicity (44). In DT-Foxp3.DTR mice, reciprocal T/DC activation occurred rapidly because of dysregulation of the entire naive T cell pool of the host. By contrast, DC activation in *Rag1*$^{-/-}$ hosts occurred more slowly, unless naive CD4 cells were injected in large numbers. However, the sequence of T/DC interaction and activation leading to effector T cell generation and DC expansion was essentially the same in both types of hosts and, with the exception of pTreg generation (see below), closely resembled typical immune responses to foreign antigens (45).

The idea that self tolerance is governed by relative B7 density implies that the capacity of Tregs to maintain self tolerance depends crucially on their capacity to modulate B7 expression on APCs. As shown here, autoreactive T cell responses developing in Treg-deficient hosts correlated closely with the raised level of B7 expression in these mice. Although modulation of B7 expression in *Rag1*$^{-/-}$ mice by Tregs is known to be CTLA-4 dependent (22), it should be noted that, in contrast to CTLA-4 deletion throughout development (5), conditional deletion of CTLA-4 in adult mice did not lead to pathological lymphadenopathy (46). Interestingly, these mice did show significant B7 up-regulation, but this was accompanied by only mild activation of normal T cells. However, Tregs were markedly expanded, so the lack of pathology in the mice may have reflected CTLA-4–independent suppression by the expanded Tregs.

A corollary of the notion that B7 levels control tolerance is that reduced expression of B7 in the thymus before T cell export to the periphery would break self tolerance. In favor of this prediction, transient perinatal B7 blockade in mice led to prominent T cell lymphoproliferation and pathology in subsequent adult life, implying lack of self tolerance when B7 levels in the periphery rose to normal levels after blockade ceased (47). A further prediction is that T cells that failed to encounter B7 in the thymus during development would be strongly reactive to APCs expressing normal B7 levels. Indeed, two studies reported that transfer of B7-deficient T cells into B7-sufficient *Rag*$^{-/-}$ hosts led to prominent lymphoproliferation and pathology (48, 49). Likewise, in a line of B7.2 (CD86) transgenic mice, the B7 transgene was highly expressed on B cells but not on DCs, which led to CD28-dependent T cell-mediated elimination of B cells (50); given that B cells are rare in the thymus, B cell elimination in the periphery may have reflected incomplete thymic tolerance to the transgene. With regard to mechanisms, the above studies were variously interpreted as reflecting the need for B7 expression for effective tolerance induction. However, the simple notion that tolerance is imprinted by the level of B7 expressed in the thymus during ontogeny and maintained by modulation of B7 density in the periphery was not mentioned.

A further corollary of the above model is that minor increases in B7 expression induced by contact with pathogens, or even danger signals from dying cells, could be sufficient to trigger activation of T cells with high affinity for self ligands. While this process could be potentially dangerous, it might also have the benefit of inducing synthesis of the background levels of IL-2 needed to sustain nTregs (51), thus allowing these cells to curtail B7 expression on DCs and thereby maintain T cell homeostasis. Would such cells remain as effector cells or differentiate into other subsets, for example, pTregs or memory T cells?

For pTregs, it is notable that self ligand-driven T-proliferative responses were accompanied by prominent pTreg generation, both in DT-Foxp3.DTR and *Rag1*$^{-/-}$ hosts, as well as in auto-MLR. pTreg cell generation was TGFβ and B7 dependent, and skewed to T cells with high self reactivity (CD5^{hi} cells) but was not seen with responses to allogeneic DCs; in Treg-depleted hosts, pTreg formation correlated with infiltration of LN with inflammatory DCs, these cells being especially stimulatory for pTreg formation in vitro. Collectively, these data on self-reactive pTregs are in close agreement with the view that pTreg generation is favored by relatively weak TCR signaling, accompanied by contact with TGFβ and a modest level of CD28 costimulation (35, 36). However, the key finding is that the self-reactive pTregs had strong suppressive function. Thus, in GF *Rag1*$^{-/-}$ hosts, ablating pTreg cell generation after transfer of naive T cells augmented infiltration of the liver with inflammatory cells.

For T memory cells, in future studies it will be important to trace the fate of T cells that become overtly autoreactive after Treg removal. Here, a key issue is whether restoring B7 levels to normal, thereby decreasing immunogenicity, causes the activated T cells to differentiate into resting memory T cells. On this point, it is notable that "virtual" memory T cells present in normal mice (52) are also found in AF mice (8) and that, in experimental models, these cells arise preferentially from high-affinity (CD5^{hi}) CD4 T cells (52). These memory T cells could arise directly from self-reactive effector cells but might also be the progeny of pTreg cells as the result of Foxp3 down-regulation (53). These questions are currently under investigation.

Materials and Methods

Detailed materials and methods are provided in *SI Appendix, Materials and Methods*.

Mice. GF *Rag1*$^{-/-}$ mice were kindly provided by Andrew Macpherson (University of Bern, Bern, Switzerland) and maintained in sterile flexible film isolators (Class Biological Clean). Foxp3-DTR mice were kindly provided by Alexander Rudensky (Memorial Sloan Kettering Cancer Center, New York) and were rederived under GF condition. For generating AF mice, GF mice were fed with antigen-free elemental liquid diet and soybean oil containing oil-soluble vitamins as described previously (8). Mouse care and experimental procedures were performed in accordance with all institutional guidelines for the ethical use of non-human animals in research protocols approved by the Institutional Animal Care and Use Committees (IACUC) of the Pohang University of Science and Technology.

Adoptive Transfer. For naive CD4 T cells, CD44^{lo} CD62L^{hi} Foxp3-GFP^{-} cells from CD90.1 or CD45.1 Foxp3-GFP mice were purified by flow cytometry sorting. After separation, donor T cells were labeled with CTV as previously described (54). Varying doses of T cells were adoptively transferred IV by retroorbital injection. For GF or AF hosts, donor T cells were manipulated aseptically, inserted into autoclaved amber glass vials capped with a silicone septum, and transferred into GF isolaters after spraying with 2% peracetic acids.

Autologous MLRs. DCs were FACS-purified from PLN by selecting for CD11c^{+} MHCII^{+} TCRβ^{-} B220^{-} Thy1.2^{-} NK1.1^{-} cells. For GF *Rag1*$^{-/-}$ mice, cells suspensions of PLN were used as a crude source of DCs (APCs). These populations of syngeneic DCs and APCs were cocultured with varying concentrations of CTV-labeled CD44^{lo} CD62L^{hi} B6 naive CD4 T cells from Foxp3-GFP mice. For MHCII blockade, clone Y3P mAb specific for I-A^{b} (Bio X Cell) was used at 10 μg/mL. For B7 blockade, clone 1G10 (Bio X Cell) and GL-1 (Bio X cell) mAbs were used at 5 μg/mL.

RNA-Seq Analysis. RNA-seq libraries were prepared by using TruSeq total RNA library (Agilent). After generation, libraries between 200 and 260 bp were enriched by Pippin automatic gel extraction system (Sage Science). Then, libraries were sequenced with MiSeq (Illumina). Log_2 of the fragments per kilobase million (FPKM) value from each sample was used for heatmap comparison. Raw data are stored at National Center for Biotechnology Information under accession number GSE121882.

Statistical Analyses. Mean and SEM values were calculated by using Prism 5 (GraphPad Software). Statistical significance was determined by unpaired two-tailed *t* tests or by one-way ANOVA followed by Newman–Keuls multiple-comparison test. *P* values less than 0.05 were considered as significant.

1. Kappler JW, Roehm N, Marrack P (1987) T cell tolerance by clonal elimination in the thymus. *Cell* 49:273–280.
2. Bennett CL, et al. (2001) The immune dysregulation, polyendocrinopathy, enteropathy, X-linked syndrome (IPEX) is caused by mutations of FOXP3. *Nat Genet* 27:20–21.
3. Kim JM, Rasmussen JP, Rudensky AY (2007) Regulatory T cells prevent catastrophic autoimmunity throughout the lifespan of mice. *Nat Immunol* 8:191–197.
4. Shevach EM (2009) Mechanisms of foxp3$^+$ T regulatory cell-mediated suppression. *Immunity* 30:636–645.
5. Wing K, et al. (2008) CTLA-4 control over Foxp3$^+$ regulatory T cell function. *Science* 322:271–275.
6. Hsieh CS, Lee HM, Lio CW (2012) Selection of regulatory T cells in the thymus. *Nat Rev Immunol* 12:157–167.
7. Haribhai D, et al. (2011) A requisite role for induced regulatory T cells in tolerance based on expanding antigen receptor diversity. *Immunity* 35:109–122.
8. Kim KS, et al. (2016) Dietary antigens limit mucosal immunity by inducing regulatory T cells in the small intestine. *Science* 351:858–863.
9. Geuking MB, et al. (2011) Intestinal bacterial colonization induces mutualistic regulatory T cell responses. *Immunity* 34:794–806.
10. Coombes JL, et al. (2007) A functionally specialized population of mucosal CD103$^+$ DCs induces Foxp3$^+$ regulatory T cells via a TGF-beta and retinoic acid-dependent mechanism. *J Exp Med* 204:1757–1764.
11. Guilliams M, et al. (2010) Skin-draining lymph nodes contain dermis-derived CD103$^-$ dendritic cells that constitutively produce retinoic acid and induce Foxp3$^+$ regulatory T cells. *Blood* 115:1958–1968.
12. Chinen T, Volchkov PY, Chervonsky AV, Rudensky AY (2010) A critical role for regulatory T cell-mediated control of inflammation in the absence of commensal microbiota. *J Exp Med* 207:2323–2330.
13. Opelz G, Kiuchi M, Takasugi M, Terasaki PI (1975) Autologous stimulation of human lymphocyte subpopulation. *J Exp Med* 142:1327–1333.
14. Lam TS, van de Meent M, Falkenburg JF, Jedema I (2015) Monocyte-derived dendritic cells can induce autoreactive CD4$^+$ T cells showing myeloid lineage directed reactivity in healthy individuals. *Eur J Immunol* 45:1030–1042.
15. Steinman RM, Witmer MD (1978) Lymphoid dendritic cells are potent stimulators of the primary mixed leukocyte reaction in mice. *Proc Natl Acad Sci USA* 75:5132–5136.
16. Scheinecker C, et al. (1998) Initiation of the autologous mixed lymphocyte reaction requires the expression of costimulatory molecules B7-1 and B7-2 on human peripheral blood dendritic cells. *J Immunol* 161:3966–3973.
17. Sprent J, Schaefer M, Lo D, Korngold R (1986) Properties of purified T cell subsets. II. In vivo responses to class I vs. class II H-2 differences. *J Exp Med* 163:998–1011.
18. Tan JT, et al. (2001) IL-7 is critical for homeostatic proliferation and survival of naive T cells. *Proc Natl Acad Sci USA* 98:8732–8737.
19. Surh CD, Sprent J (2008) Homeostasis of naive and memory T cells. *Immunity* 29: 848–862.
20. Kieper WC, et al. (2005) Recent immune status determines the source of antigens that drive homeostatic T cell expansion. *J Immunol* 174:3158–3163.
21. Hickman SP, Turka LA (2005) Homeostatic T cell proliferation as a barrier to T cell tolerance. *Philos Trans R Soc Lond B Biol Sci* 360:1713–1721.
22. Bolton HA, et al. (2015) Selective Treg reconstitution during lymphopenia normalizes DC costimulation and prevents graft-versus-host disease. *J Clin Invest* 125:3627–3641.
23. Qureshi OS, et al. (2011) Trans-endocytosis of CD80 and CD86: A molecular basis for the cell-extrinsic function of CTLA-4. *Science* 332:600–603.
24. Richards DM, et al. (2015) The contained self-reactive peripheral T cell repertoire: Size, diversity, and cellular composition. *J Immunol* 195:2067–2079.
25. Fung-Leung WP, et al. (1996) Antigen presentation and T cell development in H2-M-deficient mice. *Science* 271:1278–1281.
26. Kieper WC, Burghardt JT, Surh CD (2004) A role for TCR affinity in regulating naive T cell homeostasis. *J Immunol* 172:40–44.
27. Azzam HS, et al. (1998) CD5 expression is developmentally regulated by T cell receptor (TCR) signals and TCR avidity. *J Exp Med* 188:2301–2311.
28. Moran AE, et al. (2011) T cell receptor signal strength in Treg and iNKT cell development demonstrated by a novel fluorescent reporter mouse. *J Exp Med* 208: 1279–1289.
29. Singh N, et al. (2007) Role of CD28 in fatal autoimmune disorder in scurfy mice. *Blood* 110:1199–1206.
30. Xin L, et al. (2014) Commensal microbes drive intestinal inflammation by IL-17-producing CD4$^+$ T cells through ICOSL and OX40L costimulation in the absence of B7-1 and B7-2. *Proc Natl Acad Sci USA* 111:10672–10677.
31. Chen W, et al. (2003) Conversion of peripheral CD4$^+$CD25$^-$ naive T cells to CD4$^+$CD25$^+$ regulatory T cells by TGF-beta induction of transcription factor Foxp3. *J Exp Med* 198: 1875–1886.
32. Guo F, Iclozan C, Suh WK, Anasetti C, Yu XZ (2008) CD28 controls differentiation of regulatory T cells from naive CD4 T cells. *J Immunol* 181:2285–2291.
33. Vremec D, et al. (2011) Factors determining the spontaneous activation of splenic dendritic cells in culture. *Innate Immun* 17:338–352.
34. Sela U, Olds P, Park A, Schlesinger SJ, Steinman RM (2011) Dendritic cells induce antigen-specific regulatory T cells that prevent graft versus host disease and persist in mice. *J Exp Med* 208:2489–2496.
35. Semple K, et al. (2011) Strong CD28 costimulation suppresses induction of regulatory T cells from naive precursors through Lck signaling. *Blood* 117:3096–3103.
36. Gottschalk RA, Corse E, Allison JP (2010) TCR ligand density and affinity determine peripheral induction of Foxp3 in vivo. *J Exp Med* 207:1701–1711.
37. Sakaguchi S, Sakaguchi N, Asano M, Itoh M, Toda M (1995) Immunologic self-tolerance maintained by activated T cells expressing IL-2 receptor alpha-chains (CD25). Breakdown of a single mechanism of self-tolerance causes various autoimmune diseases. *J Immunol* 155:1151–1164.
38. Starr TK, Jameson SC, Hogquist KA (2003) Positive and negative selection of T cells. *Annu Rev Immunol* 21:139–176.
39. Metzger TC, Anderson MS (2011) Control of central and peripheral tolerance by Aire. *Immunol Rev* 241:89–103.
40. Hünig T (2012) The storm has cleared: Lessons from the CD28 superagonist TGN1412 trial. *Nat Rev Immunol* 12:317–318.
41. Langenhorst D, et al. (2018) Self-recognition sensitizes mouse and human regulatory T cells to low-dose CD28 superagonist stimulation. *Front Immunol* 8:1985.
42. Sprent J, Surh CD (2011) Normal T cell homeostasis: The conversion of naive cells into memory-phenotype cells. *Nat Immunol* 12:478–484.
43. Kowalczyk A, D'Souza CA, Zhang L (2014) Cell-extrinsic CTLA4-mediated regulation of dendritic cell maturation depends on STAT3. *Eur J Immunol* 44:1143–1155.
44. Yang Y, Wilson JM (1996) CD40 ligand-dependent T cell activation: Requirement of B7-CD28 signaling through CD40. *Science* 273:1862–1864.
45. Schoenberger SP, Toes RE, van der Voort EI, Offringa R, Melief CJ (1998) T-cell help for cytotoxic T lymphocytes is mediated by CD40-CD40L interactions. *Nature* 393: 480–483.
46. Paterson AM, et al. (2015) Deletion of CTLA-4 on regulatory T cells during adulthood leads to resistance to autoimmunity. *J Exp Med* 212:1603–1621.
47. Gao JX, et al. (2002) Perinatal blockade of b7-1 and b7-2 inhibits clonal deletion of highly pathogenic autoreactive T cells. *J Exp Med* 195:959–971.
48. May KF, Jr, et al. (2007) B7-deficient autoreactive T cells are highly susceptible to suppression by CD4$^+$CD25$^+$ regulatory T cells. *J Immunol* 178:1542–1552.
49. Paust S, Lu L, McCarty N, Cantor H (2004) Engagement of B7 on effector T cells by regulatory T cells prevents autoimmune disease. *Proc Natl Acad Sci USA* 101: 10398–10403.
50. Fournier S, Rathmell JC, Goodnow CC, Allison JP (1997) T cell-mediated elimination of B7.2 transgenic B cells. *Immunity* 6:327–339.
51. Liu Z, et al. (2015) Immune homeostasis enforced by co-localized effector and regulatory T cells. *Nature* 528:225–230.
52. Kawabe T, et al. (2017) Memory-phenotype CD4$^+$ T cells spontaneously generated under steady-state conditions exert innate T_H1-like effector function. *Sci Immunol* 2: eaam9304.
53. Zhou X, et al. (2009) Instability of the transcription factor Foxp3 leads to the generation of pathogenic memory T cells in vivo. *Nat Immunol* 10:1000–1007.
54. Martin CE, Frimpong-Boateng K, Spasova DS, Stone JC, Surh CD (2013) Homeostatic proliferation of mature T cells. *Methods Mol Biol* 979:81–106.